

# Structure of oceanic core complexes: Constraints from seafloor gravity measurements made at the Atlantis Massif

Scott L. Nooner, Glenn S. Sasagawa, Donna K. Blackman, and Mark A. Zumberge

Scripps Institution of Oceanography, La Jolla, California, USA

Received 3 February 2003; revised 25 March 2003; accepted 28 March 2003; published 30 April 2003.

[1] Using the DSV *Alvin*, the relative seafloor gravimeter ROVDOG was deployed at 18 sites on the Atlantis Massif (located at the ridge-transform intersection of the Mid-Atlantic Ridge and the Atlantis Transform Fault near 30°N, 42°W). These data along with previously collected shipboard gravity and bathymetry provide constraints on the density structure of this oceanic core complex. A series of quasi 3-D forward models suggests that symmetric east and west-dipping density interfaces bound the core of the massif with dip angles of 16°–24° in the east and 16°–28° in the west, creating a wedge with a density of 3150–3250 kg/m<sup>3</sup>. The dip angle in the east is steeper than that of the surface slope, suggesting that the detachment fault surface does not coincide with the density boundary. The resulting low-density layer is interpreted as a zone of serpentinization.

**INDEX TERMS:** 3010 Marine Geology and Geophysics: Gravity; 3094 Marine Geology and Geophysics: Instruments and techniques; 1219 Geodesy and Gravity: Local gravity anomalies and crustal structure; 8150 Tectonophysics: Plate boundary—general (3040); 9325 Information Related to Geographic Region: Atlantic Ocean. **Citation:** Nooner, S. L., G. S. Sasagawa, D. K. Blackman, and M. A. Zumberge, Structure of oceanic core complexes: Constraints from seafloor gravity measurements made at the Atlantis Massif, *Geophys. Res. Lett.*, 30(8), 1446, doi:10.1029/2003GL017126, 2003.

## 1. Introduction

### 1.1. Background

[2] This study was focused on Atlantis Massif, which is located at the eastern inside corner of the intersection between the Atlantis Transform Fault and the Mid-Atlantic Ridge (MAR) at 30°N, 42°W. Spreading parallel corrugations on the domal surface (Figure 1) are reminiscent of surface morphology at some continental core complexes in the Basin and Range and have been interpreted as characteristics of a detachment fault surface [Davis and Lister, 1988; Cann *et al.*, 1997]. Similar features have been seen at two fossil massifs along the Atlantis Fracture Zone [Blackman *et al.*, 1998; Cann *et al.*, 1997], at other places along the MAR [e.g., Cannat *et al.*, 1995; MacLeod *et al.*, 2002; Tucholke *et al.*, 2001] and elsewhere [e.g., Ranero and Reston, 1999]. The current accepted models are that these topographic highs are oceanic core complexes that form when the extension of the crust is taken up by faulting along a detachment fault rather than by plate accretion [Dick *et al.*, 1991; Mutter and Karson, 1992; Tucholke and Lin, 1994]. As the crust extends via this low angle fault, lower crustal and upper mantle rocks

are rafted to the surface. Therefore, fault rocks and ultramafic rocks that have been sampled on or near the Atlantis Massif and other hypothesized core complexes [Dick *et al.*, 1991; Cannat *et al.*, 1995; Karson, 1999; MacLeod *et al.*, 2002; Tucholke and Lin, 1994; Cann *et al.*, 1997; Tucholke *et al.*, 2001; Blackman *et al.*, 2001] are congruent with this idea.

[3] Seismic evidence of a detachment fault on the African plate capable of exhuming lower crustal or upper mantle material has been shown by Ranero and Reston [1999]. Uplift of high-density rock in this way might explain the presence of the observed gravity high on the Atlantis Massif. However, Campbell and John [1996] gave evidence for emplacement of a synextensional dike-like pluton beneath a detachment fault within the Colorado extensional corridor to explain the gravity high observed there. We use new seafloor gravity data in combination with existing sea surface gravity data to constrain a suite of 3-D forward models in order to place bounds on the geometry and value of the anomalous density in the exposed oceanic core complex at Atlantis Massif.

### 1.2. Seafloor and Sea Surface Gravity Acquisition

[4] We collected the seafloor gravity data with our seafloor gravimeter, ROVDOG (Remotely Operated Vehicle deployable Deep Ocean Gravimeter), during the Nov.–Dec., 2000 cruise of the *R/V Atlantis* as one component of MARVEL 2000. The ROVDOG was carried outside DSV *Alvin* and placed on the sea floor while an operator inside the *Alvin* controlled the instrument and observed the data collection in real time. After an observation time of 10–20 minutes the instrument was retrieved and transported to the next site. A seafloor survey taken with a single meter at an average depth of 300 m has demonstrated a precision of 28  $\mu$ Gal or better. Further technical details may be found in Sasagawa *et al.* [2003].

[5] The locations of the gravity dive sites (shown in Figure 1) form an approximately spreading-parallel line. During each of the dives, the *Alvin* gathered rock samples and stopped for gravity measurements. On average, the 18 gravity sites were spaced 557 meters apart during each of the four dives<sup>1</sup>. The sea surface gravity data that we used as part of the modeling are described in Blackman *et al.* [1998]. The uncertainty in these data are  $\sim 1.8$  mGal as indicated by the standard deviation in track crossing misfits. The location of the line is shown in Figure 1.

## 2. Data Reduction for Seafloor Gravity

[6] We corrected the gravity data for instrument drift, tides, latitude, and lithospheric cooling. We also made free water corrections to the data. The resulting uncertainties are

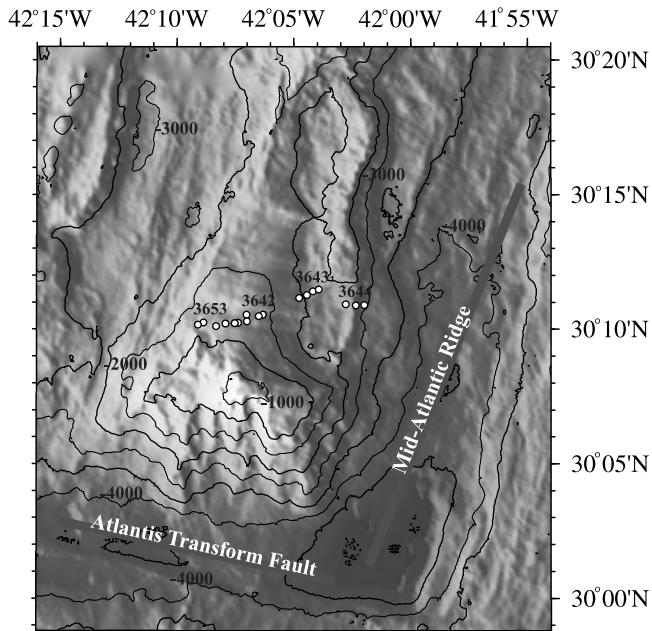


**Figure 1.** Bathymetry map with the location of seafloor gravity sites shown as white circles. Alvin dives are numbered. Notice the corrugations running from east to west near dive 3642.

summarized in Table 1. Further details can be found in Appendix 2 of the supporting material<sup>1</sup>. The accuracy in calculating the complete Bouguer anomaly from seafloor gravity data is greatly dependent on how well the shape of the seafloor itself is known. In a region like the MAR 30° N area, the terrain is often rugged and steep, making a precise terrain correction difficult. The regional bathymetry was gridded with a 100 m spacing [Blackman *et al.*, 1998], which effectively smoothes the terrain, causing discrepancies between the actual depth and that predicted by the grid. To minimize this problem, depth was measured at the gravity sites with a Paroscientific 410k pressure gauge which has demonstrated a repeatability of 3 cm in relative depth [Sasagawa *et al.*, 2003]. The free water corrections and the slab component of the terrain correction were made using these measured instrument depths. The resulting uncertainty in the slab correction is 0.004 mGal, using 2900 kg/m<sup>3</sup> as the reference density. We estimate the uncertainty in the free-water anomaly to be 0.083 mGal, whereas previous seafloor gravity studies reported uncertainties of 0.30 mGal or greater [Luyendyk, 1984; Hildebrand *et al.*, 1990; Holmes and Johnson, 1993; Ballu *et al.*, 1998; Cochran *et al.*, 1999].

[7] The RMS difference between the measured depths and those obtained from the bathymetry grid was 37 meters (150 m maximum). Shifting the survey points 100 meters west relative to the bathymetry reduced the maximum difference to about 30 m, with an RMS difference of 20 m. To determine the error in the terrain correction due to this

**Table 1.** Gravity Data Uncertainties

Error Source	Uncertainty (mGal)
Gravimeter accuracy	0.028
Tides	0.010
Latitude correction	0.071
Free water correction	0.030
Bouguer slab correction	0.004
Terrain correction	0.262
<b>Total RMS uncertainty</b>	<b>0.275</b>

unmatched depth, a Monte Carlo approach was used: normally distributed zero mean random noise (with standard deviation  $\sigma = 20$  m) was added to the bathymetric data and the terrain correction was computed. One thousand iterations of this yielded an average standard deviation of 0.262 mGal, which was adopted as the terrain correction uncertainty. This provides a better statistical estimate of uncertainty than simply computing the gravity effect of a 20 m slab, which would give an uncertainty value of about 2.4 mGal.

[8] The complete Bouguer anomaly is shown in Figure 2. The RMS uncertainty in the measurements and corrections is summarized in Table 1. The total uncertainty (0.275 mGal) is dominated by the imperfect terrain correction (0.262 mGal), demonstrating the need for more detailed bathymetry in high precision seafloor gravimetry. However, the results of this study were not strongly influenced by this issue.

### 3. Gravity Modeling

[9] Although difficult to model, small-scale features undoubtedly affect our ability to interpret the data. For instance, there is probably a continuum of density values as well as a complicated density interface boundary, such as a steepening or shallowing dip angle with depth. Due to these factors and to the inherent non-uniqueness of gravity, we approached the problem by looking only at simple, end member model geometries that neglect these second order effects. Thus we tested four types of models: homogeneous density, one-fault, cylindrical plug, and wedge.

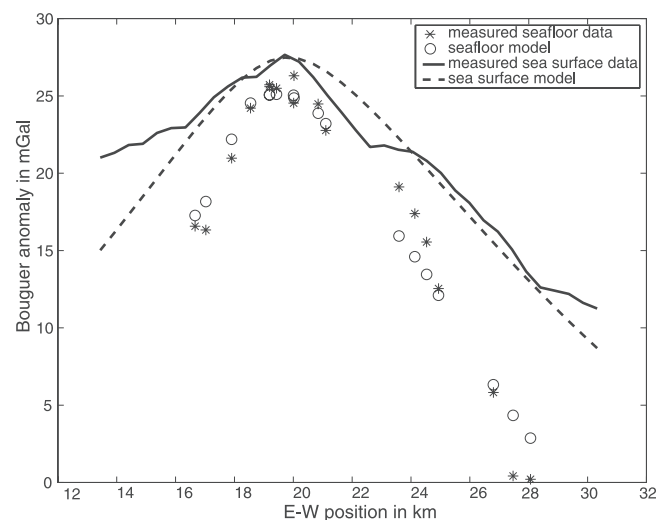


**Figure 2.** This figure shows one model fit to the seafloor and sea surface data. The dip angles bounding the high-density wedge are 16° in the east and 20° in the west;  $\Delta\rho$  is 250 kg/m<sup>3</sup>.

<sup>1</sup>Supporting material is available via Web browser or via Anonymous FTP from <ftp://ftp.agu.org>, directory "apend" (Username = "anonymous", Password = "guest"); subdirectories in the ftp site are arranged by paper number. Information on searching and submitting electronic supplements is found at [http://www.agu.org/pubs/esupp\\_about.html](http://www.agu.org/pubs/esupp_about.html).

[10] *Blackman et al.* [1998] observed that the gravity high is slightly east of the topographic high at the Atlantis Massif. Our seafloor gravity measurements confirm this. Therefore a homogeneous density model does not adequately fit both data sets, since the gravity follows topography in such a case. However, the best fitting density to this model was useful in justifying our choice for the reference density used in the Bouguer and terrain corrections ( $2900 \text{ kg/m}^3$ ). A one-fault model with one east dipping density boundary has the same difficulty as the one density model, indicating that a west-dipping boundary may be present. We also modeled a vertically oriented cylindrical plug of higher density centered on the gravity high, as has been documented in the Basin and Range [*Campbell and John*, 1996]. However, for the Atlantis Massif, this geometry requires an extremely large density contrast (greater than  $1200 \text{ kg/m}^3$ ) and a radial extent of 10–20 km for even a nominal fit to the seafloor data<sup>1</sup>. The best fitting simple model that we examined consisted of only two bodies: a high-density wedge and the surrounding terrain. The boundaries of the high-density wedge are sides sloping off to the east and to the west (Figure 3) and the transform fault to the south. The northern boundary is at  $30^{\circ}20'N$ . Tests showed that the geometry of the north and south boundaries had no significance on the model results. We swept through all combinations of east and west dip angles and wedge density contrast, requiring that the model fit both sea-surface and seafloor data.

[11] Figure 4 shows the standard deviation,  $\sigma$ , of both the seafloor and the sea surface residuals to the wedge model as a function of the east boundary dip angle and density contrast with respect to a  $2900 \text{ kg/m}^3$  reference (the dip angle in the west is held fixed at  $20^{\circ}$  for the figure). The geometries that fit both data sets best have boundary dip angles between  $16^{\circ}$ – $24^{\circ}$  in the east and  $16^{\circ}$ – $28^{\circ}$  in the west and density contrasts of  $250$ – $350 \text{ kg/m}^3$ . These ranges were obtained by requiring  $\sigma < 2 \text{ mGal}$  for both seafloor and sea surface. For the sea surface, this range was chosen because it is about the same as the uncertainty in the data. It was chosen for the seafloor because  $2 \text{ mGal}$  is approximately the small-scale variation of the data. This was determined from the residuals to a best-fitting second order polynomial. The range of eastern dip angles is slightly steeper than the angle

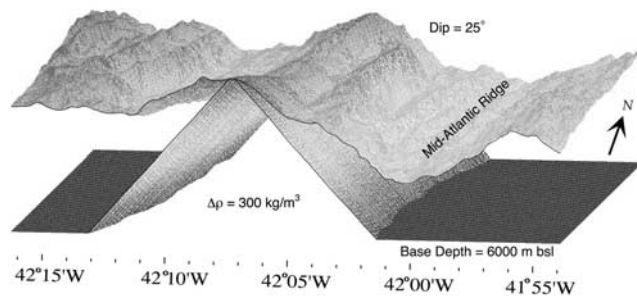


**Figure 3.** The boundaries of the high-density area form a wedge with sides sloping off to the east and to the west. We computed a suite of 3-D forward models, varying the dip angle and the density contrast of the wedge, requiring that the model fit both sea-surface and seafloor data. This wedge terminates at a depth of 6000 m below sea level (base depth). The horizontal extent of this region is 47.459 km and the vertical extent is  $\sim 5 \text{ km}$ .

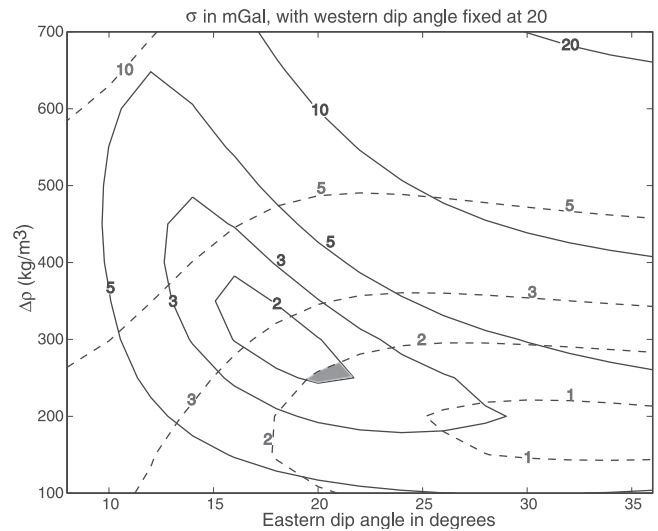


**Figure 4.** Standard deviation,  $\sigma$ , of the residuals to the model fit as a function of the eastern boundary dip angle and density contrast with respect to the  $2900 \text{ kg/m}^3$  reference. For this figure, the dip is constant at  $20^{\circ}$  in the west. Seafloor results are shown by solid lines and sea surface results are shown by dashed lines. The models that fit both data sets best, shaded region, have central high density wedge boundaries with dip angles between  $16^{\circ}$ – $24^{\circ}$  in the east and  $16^{\circ}$ – $28^{\circ}$  in the west and density contrasts of  $250$ – $350 \text{ kg/m}^3$ .

at which the corrugated seafloor dips ( $\sim 11^{\circ}$ ), indicating that the density boundary does not coincide with the fault surface. It is worth noting that the seafloor data appear to constrain the model more tightly than the sea surface data, despite the limited coverage. The seafloor data favor higher density for the wedge and a low angle boundary dip, while the sea surface data favor geometries with lower density contrast and do not constrain the fault angles well. However, a combination of the two data sets provides much better constraints than either alone.

#### 4. Discussion

[12] At the Atlantis Massif, most of the detachment fault surface is draped with pelagic ooze of some thickness, making outcrops of basement rock difficult to find. However, serpentinized peridotites and evidence of shearing are widespread across the exposed southern wall of the massif [*Blackman et al.*, 2001]. Seismic data also suggest that partially serpentinized to unaltered peridotite exist less than 1 km below the seafloor in this area [*Collins et al.*, 2001]. Consistent with this, our gravity results indicate that the core of the massif is composed of rocks with an average density of  $3150$ – $3250 \text{ kg/m}^3$ . The best fitting geometries indicate that both the east and west boundaries are more steeply dipping than the corrugated surface of the massif, as hinted at by the eastward shift of the gravity high with respect to the topographic high. This means that in the east the inferred detachment fault surface does not coincide with the density boundary, creating a strip of less dense material up to 1 km thick within the foot wall block. This is also seen in the results of the NOBEL seismic experiment [*Collins et*



al., 2001]. This low-density layer is most likely an alteration front that is sub-parallel to the detachment fault surface. Supporting this idea, rock samples from the detachment surface indicate that it is composed primarily of serpentized peridotite with some lesser amount of gabbroic material [Cann et al., 1997]. A less likely scenario is that this zone is instead magmatic in nature; i.e. rotated volcanic intrusives created during a brief magmatic phase early in the evolution of the massif, and later cut by the detachment fault, uplifted, and exposed at the surface. However, our modeling shows that large-scale dike-like intrusions beneath the detachment surface are not the cause of the observed gravity anomaly. Instead, the observed wedge-like geometry of the core is consistent with the unroofing of deep seated rock by extension and rotation along a detachment fault.

[13] The western density boundary also dips below the seafloor. Several ideas can be put forth to explain this. First, this could be a compositional boundary due to layering of a rotated crustal block. Second, the low-density region might be due to the presence of a rider block that was carried eastward during extension along the detachment. Finally, the zone could be a continuation of the alteration front associated with the detachment fault surface. The breakaway zone is thought to be several kilometers west of the modeled area. Our limited gravity coverage in the west does not allow us to make any conclusive statements regarding structure of this area.

[14] These interpretations are consistent with the presence of a detachment fault. Although some seismic studies have been done in the region [Collins and Detrick, 1998; Collins et al., 2001], more detailed results could help further constrain dip angles and elastic properties of the massif, allowing us to better define the density contrast and geometry. Because of the limited coverage of our single-profile seafloor data set it is not beneficial to test more complicated models, although it is likely that there is some small scale surface density variability as well as subsurface density structure. In fact, because of the limited extent, the gravity data provide little north-south constraints on the structure. These come mostly from the morphology of the region. Further studies of these structures with more extensive gravity measurements, seismic studies, and drilling will help us to understand these interesting extensional regions.

[15] **Acknowledgments.** We thank the shipboard participants on cruise AT03-60, the officers, crew and pilots of the RV *Atlantis* and DSV *Alvin*, Statoil for the loan of ROVDOG, Robert L. Parker for software, and Eric Husmann for instrument preparation, and the reviewers for their suggestions.

## References

Ballu, V., J. Dubois, C. Deplus, M. Diamant, and S. Bonvalot, Crustal structure of the Mid-Atlantic Ridge south of the Kane Fracture Zone from seafloor and sea surface gravity data, *J. Geophys. Res.*, **103**, 2615–2631, 1998.

- Blackman, D. K., J. R. Cann, B. Janssen, and D. K. Smith, Origin of extensional core complexes: Evidence from the Mid-Atlantic Ridge at Atlantis Fracture Zone, *J. Geophys. Res.*, **103**, 21,315–21,333, 1998.
- Blackman, D. K., D. S. Kelley, J. A. Karson, and MARVEL2000, New seafloor maps and samples from the Mid-Atlantic Ridge 30N oceanic core complex, *Eos Trans. AGU*, **82**(47), Fall Meet. Suppl., 2001.
- Campbell, E. A., and B. E. John, Constraints on extension-related plutonism from modeling of the Colorado River gravity high, *Geolog. Soc. Am. Bulletin*, **108**, 1242–1255, 1996.
- Cann, J. R., D. K. Blackman, D. K. Smith, E. McAllister, B. Janssen, S. Mello, E. Avgerinos, A. R. Pascoe, and J. Escartin, Corrugated slip surfaces formed at ridge-transform intersections on the Mid-Atlantic Ridge, *Nature*, **385**, 329–332, 1997.
- Cannat, M., C. Mevel, M. Maia, C. Deplus, C. Durand, P. Gente, P. Agnirier, A. Belarouchi, G. Dubuisson, E. Humler, and J. Reynolds, Thin crust, ultramafic exposures, and rugged faulting patterns at the Mid-Atlantic Ridge (22°–24°N), *Geology*, **23**, 49–52, 1995.
- Cochran, J. R., D. J. Fornari, B. J. Coakley, R. Herr, and M. A. Tivey, Continuous near-bottom gravity measurements made with a BGM-3 gravimeter in DSV *Alvin* on the East Pacific Rise Crest near 9°31'N and 9°50'N, *J. Geophys. Res.*, **104**, 10,841–10,861, 1999.
- Collins, J., and R. S. Detrick, Seismic structure of the Atlantis Fracture Zone megamullion, a serpentized untramafic massif, *Eos Trans. AGU*, **79**, F800, 1998.
- Collins, J. A., B. E. Tucholke, and J. Canales, Structure of Mid-Atlantic Ridge megamullions from seismic refraction experiments and multichannel seismic reflection profiling, *Eos Trans. AGU*, **82**, Fall Meet. Suppl., F1100, 2001.
- Davis, G. A., and G. S. Lister, Detachment faulting in continental extension: perspectives from the southwestern U.S. cordillera, *Spec. Pap. Geol. Soc. Am.*, **218**, 133–159, 1988.
- Dick, H. J. B., P. S. Meyer, S. Bloomer, S. Kirby, D. Stakes, and C. Mawer, Lithostratigraphic evolution of an in-situ section of oceanic layer 3, in Von Herzen and Robinson et al., *Proc. ODP Sci. Res.*, **118**, 439–538, 1991.
- Hildebrand, J. A., J. M. Stevenson, P. T. C. Hammer, M. A. Zumberge, and R. L. Parker, A seafloor and sea surface gravity survey of Axial Volcano, *J. Geophys. Res.*, **95**, 12,751–12,763, 1990.
- Holmes, M. L., and H. P. Johnson, Upper crustal densities derived from seafloor gravity measurements: northern Juan de Fuca Ridge, *Geophys. Res. Lett.*, **20**, 1871–1874, 1993.
- Karson, J. A., Geological investigation of a lineated massif at the Kane Transform Fault: implications for oceanic core complexes, *Phil. Trans. Roy. Soc. Lond., A*, **357**, 713–736, 1999.
- Luyendyk, B. P., On-bottom gravity profile across the East Pacific rise crest at 21° north, *Geophysics*, **49**, 2166–2177, 1984.
- MacLeod, C. J., J. Escartin, D. Banerji, G. J. Banks, M. Gleeson, D. H. B. Irving, R. M. Lilly, A. M. McCaig, Y. Niu, S. Allerton, and D. K. Smith, Direct geological evidence for oceanic detachment faulting: The Mid-Atlantic Ridge, 15°45'N, *Geology*, **30**, 879–882, 2002.
- Mutter, J. C., and J. A. Karson, Structural processes at slow spreading ridges, *Science*, **257**, 627–634, 1992.
- Ranero, C. R., and T. J. Reston, Detachment faulting at ocean core complexes, *Geology*, **27**, 983–986, 1999.
- Sasagawa, G., W. Crawford, O. Eiken, S. Nooner, T. Stenvold, and M. Zumberge, A new seafloor gravimeter, *Geophysics*, in press, 2003.
- Tucholke, B. E., and J. Lin, A geological model for the structure of ridge segments in slow spreading ocean crust, *J. Geophys. Res.*, **99**, 11,937–11,958, 1994.
- Tucholke, B. E., K. Fujioka, T. Ishihara, G. Hirth, and M. Kinoshita, Submersible study of an oceanic megamullion in the central North Atlantic, *J. Geophys. Res.*, **106**, 16,145–16,161, 2001.

D. K. Blackman, S. L. Nooner, G. S. Sasagawa, and M. A. Zumberge, Scripps Institution of Oceanography, La Jolla, CA 92093-0225, USA. (snooner@ucsd.edu)